Constitutive relation of viscoelastic dielectric elastomer

Junshi Zhang,[1,2] Hualing Chen,[1,3,a)] Junjie Sheng,[1,3] Lei Liu,[1,3] Yongquan Wang,[3] and Shuhai Jia[3]
[1)] *State Key Laboratory for Strength and Vibration of Mechanical Structures, Xi'an Jiaotong University, Xi'an 710049, China*
[2)] *School of Aerospace, Xi'an Jiaotong University, Xi'an 710049, China*
[3)] *School of Mechanical Engineering, Xi'an Jiaotong University, Xi'an 710049, China*

(Received 21 July 2013; accepted 21 August 2013; published online 10 September 2013)

Abstract In this paper, we present a modified model describing the constitutive relation of viscoelastic dielectric elastomer (DE). The uniform uniaxial tension-recovery experiment was carried out at different stretching rates. Based on Yeoh hyper-elastic model, model-fitting approach is put forward to obtain the relationship between parameters of Yeoh model and stretching rate, thus the modified model was obtained. From the approximate relationship between harmonic motion and uniform reciprocating motion, the stress–strain curve in the recovery process was also identified through the hysteresis between stress and strain. The modified model, with concise form and evident physical concept, can describe the strong nonlinear behavior between deformation and mechanical stress of the material in a common stretching rate range (from $0.01\,\mathrm{s}^{-1}$ to $0.8\,\mathrm{s}^{-1}$ at least). The accuracy and reliability of the modified model was examined. [doi:10.1063/2.1305411]

Keywords dielectric elastomer, Yeoh model, modified model, stretching rate, hysteresis

Dielectric elastomer (DE), which belongs to the group of electro-active polymers (EAPs), generally refers to a kind of emerging material (mostly derived from acrylics and silicones) which can exhibit large dimensional changes upon electrical stimulation.[1–3] Due to its high-strain responsive performance together with other desirable properties, such as low cost, high energy density, large degrees of compliance, so far a variety of promising DE actuators (DEAs) have been significantly developed, including biomimetic robots, optical switches, micro-pumps (or valves), micro-motors, smart skin, and tactile display, etc.[4–6]

The mechanical deformation behavior of super-elastic material is usually described by strain energy density function. In the process of mechanical research of DE, there are several commonly used super-elastic models to describe relationship between deformation and energy, such as Mooney–Rivlin model,[7] Yeoh model,[8] Ogden model,[9] and Gent model.[10] Mooney–Rivlin model is widely used in the calculation of the elastic deformation, assuming that the shear modulus does not vary with the strain. Yeoh model uses higher order of left Cauchy–Green deformation tensor or the first principal invariant, so it can more accurately describe medium deformation to large deformation of the material. According to the demand and experimental data, the order of Ogden model can be freely selected, so this model can be carried out with varying degrees of transformation depending on conditions. Gent model considers the stretching limits of molecular chain and is able to account for the phenomenon of stress-stiffening in the case of large deformation.

Viscoelasticity, an inherent property of all high molecular polymers (including DE materials), could largely affect their performance. Previous studies showed that the viscoelastic damping of dielectric elastomer has strong nonlinearity under medium to large deformation. It is difficult to be described comprehensively by the conventional strain energy model of hyper-elastic material. As a kind of macromolecule polymer, DE's hyper-elastic property has been widely reported.[11–14] However, investigations on its viscoelasticity, which plays a significant role in the performance of DE devices, seem to be far insufficient yet. Earlier publications have presented some quasi-linear viscoelastic models,[15–17] which are more appropriate for describing the mechanical properties of DE films under relatively low stretches (some applications, however, can use stretch ratio of up to 4 or even larger) and static viscoelastic behaviors such as stress relaxation and creep. Another approach was once presented in Ref. 12, where a time function, i.e., Prony series, was introduced into a hyper-elastic strain energy potential (e.g., Orgen, Mooney–Rivlin, or Yeoh model) to describe DE time-dependent behaviors under large extensions. However, it still seems complicated in form and thus difficult to be used in practical design. In 2007, the tension-recovery experiment of DE material was carried out by Plante and Dubowsky,[18] and the experimental results were fitted by Bergström–Boyce model, explaining the impact of viscoelasticity on the output force of DE actuator. In 2011, Zhao et al.[19] studied viscoelasticity with the rheological model of two springs and a dashpot, and fitted the experimental data in Ref. 18 based on this model. The results showed that this viscoelastic model is quite accurate with the stretching rate of $3.3\times10^{-4}\,\mathrm{s}^{-1}$, but when stretching rate is above $9.4\times10^{-2}\,\mathrm{s}^{-1}$, the difference between numerical simulation and experimental data increases gradually. Thus, a constitutive model of viscoelastic dielectric elastomer with wider applicability is necessary and expected.

[a)] Corresponding author. Email: hlchen@mail.xjtu.edu.cn.

As mentioned above, a number of hyper-elastic strain energy models have been developed to describe the mechanical constitutive behaviors of DE, all of which are obtained using experimental data fitting. In this paper, Yeoh super-elastic model is selected, which gives the strain energy density function W as

$$W = C_1(I_1 - 3) + C_2(I_1 - 3)^2 + C_3(I_1 - 3)^3, \quad (1)$$

where I_1 is the first principal invariant, defined as $I_1 = \lambda_1^2+\lambda_2^2+\lambda_3^2$, with λ_i (i=1, 2, 3) denoting the stretch ratio in three principal directions, respectively. λ_i is then related to the material dimensions by $\lambda_i = L_i/L_{i0}$ with L_i and L_{i0} representing the stretched and initial length of the film in the direction i. C_1, C_2, C_3 are material parameters determined by the uniaxial tensile test at specific temperature and stretching rate. C_1 generally stands for the initial shear modulus at small stretch ratio. C_2 (negative) and C_3 (positive), describe the material's nonlinear stiffness characteristics that when the deformation level increases, the material will become softer at first but get stiffer afterwards.

Due to the incompressibility of DE material, that is, $\lambda_1\lambda_2\lambda_3 = 1$, when the film is stretched uniaxially, stretch ratios in the three directions satisfy the following relationship

$$\lambda_2 = \lambda_3 = \frac{1}{\sqrt{\lambda_1}}. \quad (2)$$

We could obtain the Cauchy stress (true stress) based on the Yeoh model in the tensile direction (direction 1)[8,11]

$$\sigma_1 = 2(\lambda_1^2 - \frac{1}{\lambda_1})\Big[C_1 + 2C_2(\lambda_1^2 + \frac{2}{\lambda_1} - 3) + 3C_3(\lambda_1^2 + \frac{2}{\lambda_1} - 3)^2\Big]. \quad (3)$$

To study the viscoelastic properties of DE, uniform uniaxial tension-recovery test is carried out at different stretching rates. DE material used here is very high bond (VHB) 4 910 film manufactured by 3M, belongs to polyacrylate. The initial length, width, and thickness of the sample are 15 mm, 10 mm, and 1 mm, respectively. The Tytron 250 micro force testing system produced by MTS Company (USA) is employed in the experiment, as shown in Fig. 1.

The experiment is carried out at room temperature of 30°C. This sample is uniaxially stretched up to 60 mm at different stretching rates (from 0.01 s^{-1} to 0.8 s^{-1} respectively), with the maximum stretch ratio of 4.

Figure 2 shows parts of the true stress-stretch ratio curves at different stretching rates. We can see that stretching rate has a strong influence on the stress. For the same stretch ratio, both tension stress and recovery stress increase with increasing stretching rate. And at all of the stretching rates, there obviously exist nonlinear dependencies between the stress and stretch ratio. Furthermore, tension stress and recovery stress do not overlap, but show a hysteresis loop. All of these indicate the presence of complex viscoelasticity of DE.

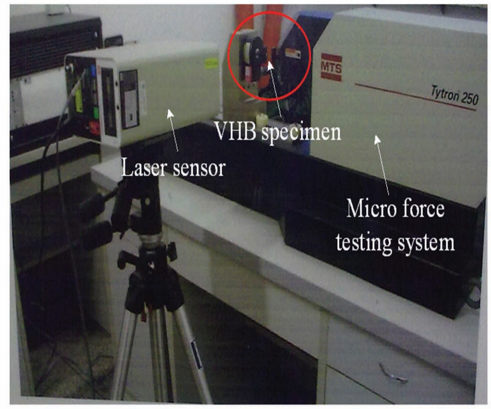

Fig. 1. Uniaxial tensile test equipment—Tytron 250 micro force testing system.

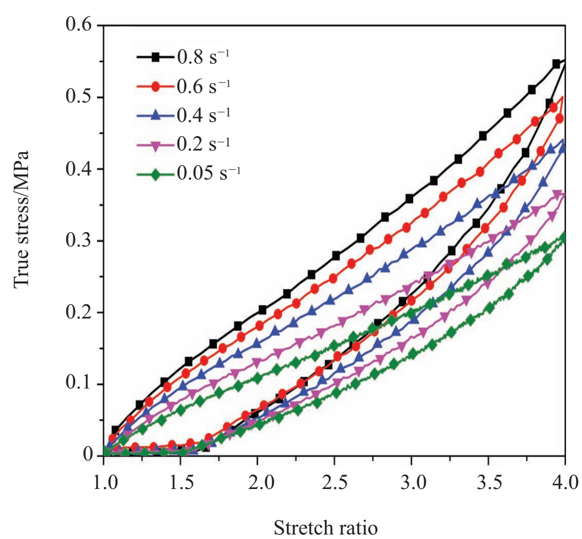

Fig. 2. True stress against stretch ratio at different stretching rates.

If each curve of tension stress in Fig. 2 is fitted by using Eq. (3), different stretching rates will correspond to the different material parameters.

Figure 3 plots material parameters obtained from the respective nonlinear fitting versus the stretching rate. As can be seen, monotonic increase of the numerical value of model parameters can be found with the increase of stretching rate. The reason may be that, since DE is a viscoelastic material, the larger stretching rate will make the increase of viscous resistance during the tensile process, therefore lead to an increase of the model parameters. Exponential model is used to describe the relation between the model parameters and the stretching rate as

$$C_i(\dot{\lambda}_1) = a_i\dot{\lambda}_1^{b_i} + c_i, \; i = 1, 2, 3, \quad (4)$$

where a_i, b_i, and c_i are coefficients to be determined.

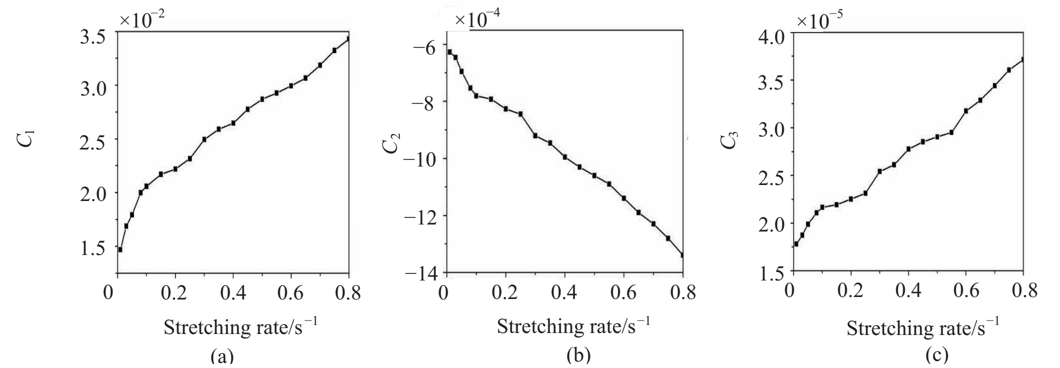

Fig. 3. Relationship between parameters of Yeoh model and stretching rate.

Using the data of model parameters obtained after fitting and stretching rate, by fitting them with Eq. (4) we could obtain the following equations

$$C_1(\dot{\lambda}_1) = 0.022\,04\dot{\lambda}_1^{0.591\,6} + 0.014\,09, \tag{5a}$$

$$C_2(\dot{\lambda}_1) = (-8.240\,6 \times 10^{-4})\dot{\lambda}_1^{0.932\,4} -6.419\,3 \times 10^{-5}, \tag{5b}$$

$$C_3(\dot{\lambda}_1) = (2.293\,8 \times 10^{-5})\dot{\lambda}_1^{1.078\,7} +1.868\,7 \times 10^{-5}. \tag{5c}$$

Thus the modified Yeoh model, which is actually an implicit function of the stretching rate, can be expressed as

$$\sigma_1 = 2\Big(\lambda_1^2 - \frac{1}{\lambda_1}\Big)\Big[C_1(\dot{\lambda}_1) + 2C_2(\dot{\lambda}_1)\Big(\lambda_1^2 + \frac{2}{\lambda_1} - 3\Big) +3C_3(\dot{\lambda}_1)\Big(\lambda_1^2 + \frac{2}{\lambda_1} - 3\Big)^2\Big]. \tag{6}$$

Based on hysteresis between stress and strain, next we determine the stress–strain curve in the recovery process by using Eq. (6). In a uniform tension-recovery cycle, the stress will always keep ahead of the stretch ratio, presenting an enclosed hysteresis loop. During the tensile process, the work done by external force on the polymer system, U_1, is

$$U_1 = U + \Delta U_1, \tag{7}$$

where U denotes the stored elastic energy, ΔU_1 denotes the dissipated energy to overcome the internal friction in the tensile process.

When DE is in the recovery process, the total energy of the polymer system is U (the stored elastic energy in the tensile process)

$$U = U_2 + \Delta U_2, \tag{8}$$

where U_2 denotes the work done by polymer system on external environment, ΔU_2 denotes the dissipated energy to overcome the internal friction in the recovery process. Since DE is in a uniform tension-recovery, so we assume that $\Delta U_1 = \Delta U_2$.

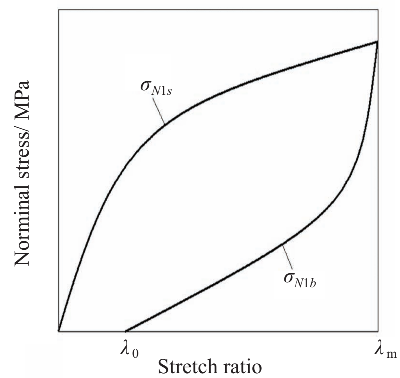

Fig. 4. Schematic nominal stress versus stretch ratio.

As shown in Fig. 4, σ_{N1s} denotes the tension stress, σ_{N1b} denotes the recovery stress, λ_0 denotes the residual stretch ratio, λ_{m} denotes the maximum stretch ratio. During a uniform tension-recovery cycle, the dissipated energy due to the internal friction is

$$\Delta U = U_1 - U_2 = V\int_1^{\lambda_{\mathrm{m}}} \sigma_{N1s}\mathrm{d}\lambda - V\int_{\lambda_0}^{\lambda_{\mathrm{m}}} \sigma_{N1b}\mathrm{d}\lambda = \Delta U_1 + \Delta U_2 = 2\Delta U_1, \tag{9}$$

where V denotes the volume of polymer material.

From the polymer physics we can obtain

$$\tan\delta = \frac{\Delta U_1}{U} = \frac{\Delta U_1}{U_1 - \Delta U_1}, \tag{10}$$

where δ denotes the lag angle between stress and strain.

To facilitate the use of lag angle, here we approximate the uniform tension-recovery motion as the first half cycle of a harmonic motion, as shown in Fig. 5, where the solid line represents the uniform tension-recovery motion and the dash line represents the harmonic motion. The determination of stress–strain curve in the recovery process is divided into two steps, the first step is to obtain the lag angle δ for each given stretching rates by using Eq. (10), with experimental data in

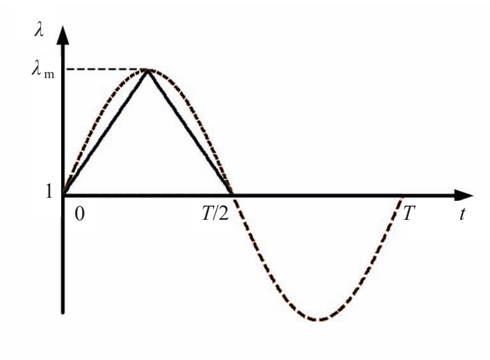

Fig. 5. Approximate relation between uniform motion (solid line) and harmonic motion (dash line).

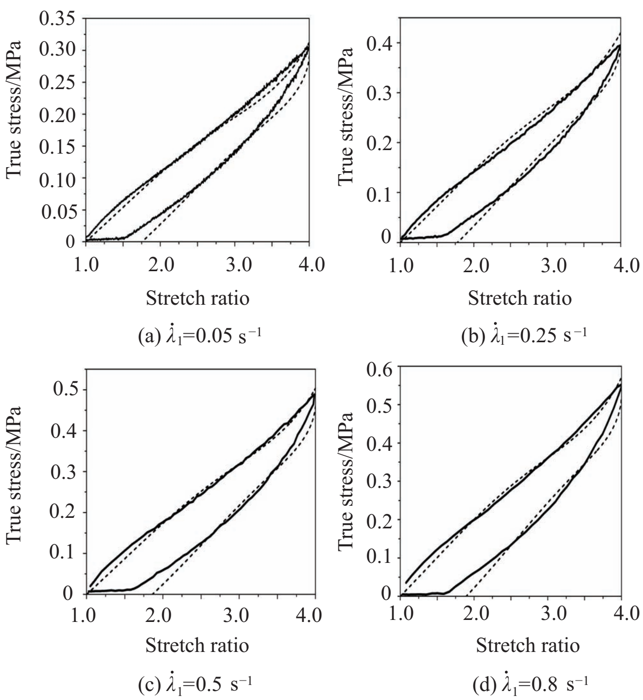

Fig. 6. Comparison of hysteresis loops between the theoretical (dash line) and experimental (solid line) results.

uniform tension-recovery tests. In the second step, using the corresponding lag relationship between stress and strain, thus the stress–strain curve in the recovery process can be obtained.

In order to validate the correctness of the derived modified model, based on a few uniaxial tension-recovery test sequences with different stretching rates, we compared them with the calculation results from the theoretical modified model by using Eq. (6). Figure 6 gives parts of the comparison of the hysteresis loops separately obtained from experimental tests and theoretical calculations at several stretching rates, still with the maximum stretch ratio being 4. As can be seen, the parameters of Yeoh model only coming from fit of unidirectional tensile procedure, can also well depict the hysteretic behaviors of DE film in its recovery, bringing a good agreement with the experimental results.

This paper presented the constitutive relation of viscoelastic dielectric elastomer based on generalized Yeoh model. By experimentally exploring the dependence of parameters of Yeoh model on stretching rates, and approximating the harmonic motion as uniform reciprocating motion, the constitutive relation of viscoelastic dielectric elastomer is ultimately obtained. The modified model, with concise form and evident physical concept, can describe the strong nonlinear behavior between the large deformation and mechanical stress of the material in a common stretching rate range (from 0.01 s^{-1} to 0.8 s^{-1} at least). The accuracy of the model is completely acceptable for practical engineering applications.

The work was supported by the Doctoral Fund of Ministry of Education of China (20120201110030).

1. R. Pelrine, R. Kornbluh, Q. B. Pei, et al. Science **287**, 836 (2000).
2. R. Pelrine, R. Kornbluh, and G. Kofod, Adv. Mater. **16**, 1223 (2000).
3. Z. G. Suo, Acta. Mech. Solida. Sin. **23** 549 (2010).
4. H. Choi, S. Ryew, K. Jung, et al., IEEE Int. Conf. on Robotics and Automation **3**, 3212 (2002).
5. J. S. Plante and S. Dubowsky, Smart Mater. Struct. **16**, 227 (2007).
6. A. Rajamani, M. D. Grissom, C. D. Rahn, et al., IEEE/ASME Transactions on Mechanics **13**, 117 (2008).
7. M. Mooney, J. Appl. Phys. **11**, 582 (1940).
8. O. H. Yeoh, Rubber Chem. Technol. **63**, 792 (1990).
9. A. Dorfmann and R. Ogden, Acta. Mech. **174**, 167 (2005).
10. M. Boyce and E. Arruda, Rubber Chem. Tech. **73**, 504 (2000).
11. M. Wissler and E. Mazza, Sensor. Actuat. A-phys. **120**, 184 (2005).
12. L. Patrick, K. Gabor, and M. Silvain, Sensor. Actuat. A-phys. **135**, 748 (2007).
13. S. J. A. Koh, X. H. Zhao, and Z. G. Suo, Appl. Phys. Lett. **94**, 262902 (2009).
14. Y. J. Liu, L. W. Liu, Z. Zhang, et al., Europhys. Lett. **90**, 36004 (2010).
15. C. Jean-Mistral, S. Basrour, and J. J. Chaillout, Smart Mater. Struct. **19**, 105006 (2010).
16. M. Wissler and E. Mazza, Smart Mater. Struct. **14**, 1396 (2005).
17. E. Yang, M. Frecker, and E. Morckensturm, Proc. of SPIE **5759**, 82 (2005).
18. J. S. Plante and S. Dubowsky, Sensor. Actuat. A-phys. **137**, 96 (2007).
19. X. H. Zhao, S. J. A. Koh, and Z. G. Suo, Int. J. Appl. Mech. **3**, 203 (2011).